Electronic Supplementary Material (ESI) for Analytical Methods.

Supporting Information

Solvation Effect Enabled Visualized Discrimination of Multiple Metal Ions

Yang Cheng,[a,b] Yuan Liu,[a,*] Jiguang Li,[a] Yudong Li,[a] Da Lei,[a] Dezhong Li,[a] Xincun Dou[a,b,*]

[a] Xinjiang Key Laboratory of Trace Chemical Substances Sensing, Xinjiang Technical Institute of Physics and Chemistry, Chinese Academy of Sciences, Urumqi 830011, China

[b] Center of Materials Science and Optoelectronics Engineering, University of Chinese Academy of Sciences, Beijing 100049, China

* Corresponding author: liuyuan@ms.xjb.ac.cn; xcdou@ms.xjb.ac.cn

Experiments

Theoretical computation details

Based on density functional theory (DFT), PBE0[1] exchange-correlation functional with Grimme's DFT D3(BJ)[2, 3] and def2-SVP[4, 5] basis set were used to optimize the molecular structures at ground state. A further frequency calculation at the same level of theory was also performed at the optimized geometries to ensure that the located stationary points do not have any imaginary frequency. Based on time-dependent density functional theory (TD-DFT), PBE0 exchange-correlation functional and def2-SVP basis set were used to optimize the molecular structures of the lowest singlet excited state (S1) and calculate the vertical emission energy with the solvent settings of DMF or THF. The solvation free energies of the APT probe were calculated by the difference of the single point energy between the solution phase condition and the gas phase condition at the M05-2X[6] with def2-TZVPP[5].The polarizable continuum model[7] was employed to take into account the effects of the solvents. All calculations are based on Gaussian 09[8] program package, all wave function analysis include hole-electron analysis[9] were processed by the Multiwfn[10] software, and the image data were rendered by VMD[11].

Synthesis process of product of APT-Cu(II)

2 mL anhydrous DMF, 0.2 mmol (0.0390 g) 5-amino-1, 10-phenanthroline (APT), and 0.2 mmol (0.0319 g) anhydrous $CuSO_4$ were mixed in a sealed reaction container and stirred overnight at 80 ℃. The purified filtrate was obtained after reaction. HRMS (ESI) calcd for $C_{24}H_{18}N_6Cu^{2+}$ m/z M^+: 453.0878; found: 453.0884.

Preparation of the APT probe

9.8 mg APT was dissolved in different solvents (dimethyl sulfoxide-DMSO, DMF, MeCN, acetone, THF, the mixture of DMF/H_2O with a ratio of 1:2) to receive the probe solution with a concentration of 0.1 mM, respectively.

Preparation of the metal ions solutions

$CuSO_4$ stock solution: 16 mg $CuSO_4$ powder was dissolved in 10 mL deionized water to prepare the $CuSO_4$ stock solution with a concentration of 10 mM. Then the solution was diluted with deionized water to obtain the $CuSO_4$ solutions with various concentrations. $ZnCl_2$ stock solution: 13.6 mg $ZnCl_2$ powder was dissolved in 10 mL deionized water to prepare the $ZnCl_2$ stock solution with a concentration of 10 mM. Then the solution was diluted with deionized water to obtain the $ZnCl_2$ solutions with various concentrations. $CdCl_2$ stock solution: 18.4 mg $CdCl_2$ powder was dissolved in 10 mL deionized water to prepare the $CdCl_2$ stock solution with a concentration of 10 mM. Then the solution was diluted with deionized water to obtain the $CdCl_2$ solutions with various concentrations. $AlCl_3$ stock solution: 13.3 mg $AlCl_3$ powder was dissolved in 10 mL deionized water to prepare the $AlCl_3$ stock solution with a

concentration of 10 mM. Then the solution was diluted with deionized water to obtain the $AlCl_3$ solutions with various concentrations.

Studies of solvation effect on the APT probe and its complexation towards metal ions

The fluorescence spectra of 0.1 mM probe in different solvents (DMSO, DMF, MeCN, acetone, THF) were measured on the Edinburgh FLS1000 fluorescence spectrophotometer with settings of slit=1.5 nm, λ_{ex}= 365 nm. Then, 20 μL 10 mM $CuSO_4$, $ZnCl_2$, $CdCl_2$ and $AlCl_3$ solutions were added into 1.98 mL 0.1 mM APT probe in DMF, THF and DMF/H_2O (*v*/*v*=1:2), respectively. The fluorescence spectra were measured on the Edinburgh FLS1000 fluorescence spectrophotometer with different settings, for DMF systems: slit=1.5 nm, λ_{ex}=365 nm; for THF systems: slit=1.5 nm, λ_{ex}=365 nm; for DMF/H_2O (*v*/*v*=1:2) system: slit=1.5 nm, λ_{ex}=305 nm. All fluorescent images of the probe solutions before and after the addition of metal ions were obtained by an iPhone 12.

Stability study

20 μL 1 mM $CuSO_4$ solution was added into 1.98 mL 10 μM APT probe in DMF on each single day with a duration of 10 days. The fluorescence spectra for the probe before and after the addition of $CuSO_4$ solution were measured on the Edinburgh FLS1000 fluorescence spectrophotometer with the setting of slit=1.5 nm, λ_{ex}=365 nm. All fluorescent images were obtained by an iPhone 12. 20 μL 1 mM $ZnCl_2$ solution was added into 1.98 mL 10 μM APT probe in THF on each single day with a duration of 10 days. The fluorescence spectra for the probe before and after the addition of $ZnCl_2$ solution were measured on the Edinburgh FLS1000 fluorescence spectrophotometer with the setting of slit=1.5 nm, λ_{ex}=365 nm. All fluorescent images were obtained by an iPhone 12. 20 μL 1 mM $CdCl_2$ solution was added into 1.98 mL 10 μM APT probe in THF on each single day with a duration of 10 days. The fluorescence spectra for the probe before and after the addition of $CdCl_2$ solution were measured on the Edinburgh FLS1000 fluorescence spectrophotometer with the setting of slit=1.5 nm, λ_{ex}=365 nm. All fluorescent images were obtained by an iPhone 12. 20 μL 3 mM $AlCl_3$ solution was added into 1.98 mL 30 μM APT probe in DMF/H_2O (*v*/*v*=1:2) on each single day with a duration of 10 days. The fluorescence spectra for the probe before and after the addition of $AlCl_3$ solution were measured on the Edinburgh FLS1000 fluorescence spectrophotometer with the setting of slit=2 nm, λ_{ex}=305 nm. All fluorescent images were obtained by an iPhone 12.

Evaluation on response time

20 μL 1 mM $CuSO_4$ solution was added into 1.98 mL 10 μM APT probe in DMF, 20 μL 1 mM $ZnCl_2$ solution was added into 1.98 mL 10 μM APT probe in THF, 20 μL 1 mM $CdCl_2$ solution was added into 1.98 mL 10 μM APT probe in THF, and 20 μL 3 mM $AlCl_3$ solution was added into 1.98 mL 30 μM APT probe in DMF/H_2O (*v*/*v*=1:2). The response time was recorded based on the video taken by an iPhone 12,

then, the instant response image was extracted for evaluate the response time of the APT probe towards individual metal ions.

Practical analysis of the simulated tap-water and sewage

Preparation and analysis of the tap-water samples

10 mM $CuSO_4$ stock solution was diluted by the tap-water with the concentrations of 0.4, 0.6 and 1 mM. Then, 20 μL $CuSO_4$ spiked tap-water sample was added into 1.98 mL 10 μM APT probe in DMF. 10 mM $ZnCl_2$ stock solution was diluted by the tap-water with the concentrations of 0.3, 0.5 and 1.5 mM. Then, 20 μL $ZnCl_2$ spiked tap-water sample was added into 1.98 mL 10 μM APT probe in THF. 10 mM $CdCl_2$ stock solution was diluted by the tap-water with the concentrations of 0.4, 0.8 and 1.2 mM. Then, 20 μL $CdCl_2$ spiked tap-water sample was added into 1.98 mL 10 μM APT probe in THF. 10 mM $AlCl_3$ stock solution was diluted by the tap-water with the concentrations of 0.6, 0.9 and 1.5 mM. Then, 20 μL $AlCl_3$ spiked tap-water sample was added into 1.98 mL 30 μM APT probe in DMF/H_2O (v/v=1:2). The fluorescence spectra for the APT probe before and after detecting the $CuSO_4$, $ZnCl_2$ and $CdCl_2$ spiked tap-water samples were measured on the Edinburgh FLS1000 fluorescence spectrophotometer with the setting of slit=1.5 nm, λ_{ex}=365 nm. For the $AlCl_3$ spiked tap-water samples, the fluorescence spectra were measured on the Edinburgh FLS1000 fluorescence spectrophotometer with the setting of slit=2 nm, λ_{ex}=305 nm.

Preparation and analysis of the sewage samples

10 mM $CuSO_4$ stock solution was diluted by the sewage with the concentrations of 0.3, 0.5 and 1 mM. Then, 20 μL $CuSO_4$ spiked sewage sample was added into 1.98 mL 10 μM APT probe in DMF. 10 mM $ZnCl_2$ stock solution was diluted by the sewage with the concentrations of 0.2, 0.6 and 2 mM. Then, 20 μL $ZnCl_2$ spiked sewage sample was added into 1.98 mL 10 μM APT probe in THF. 10 mM $CdCl_2$ stock solution was diluted by the sewage with the concentrations of 0.4, 0.7 and 1.2 mM. Then, 20 μL $CdCl_2$ spiked sewage sample was added into 1.98 mL 10 μM APT probe in THF. 10 mM $AlCl_3$ stock solution was diluted by the sewage with the concentrations of 0.8, 1.6 and 3 mM. Then, 20 μL $AlCl_3$ spiked sewage sample was added into 1.98 mL 30 μM APT probe in DMF/H_2O (v/v=1:2). The fluorescence spectra for the APT probe before and after detecting the $CuSO_4$, $ZnCl_2$ and $CdCl_2$ spiked sewage samples were measured on the Edinburgh FLS1000 fluorescence spectrophotometer with the setting of slit=1.5 nm, λ_{ex}=365 nm. For the $AlCl_3$ spiked sewage samples, the fluorescence spectra were measured on the Edinburgh FLS1000 fluorescence spectrophotometer with the setting of slit=2 nm, λ_{ex}=305 nm.

Sensing response of the portable sensing chip towards metal ions

The A, B and C sensing units of the customized portable sensing chip were filled with 0.5 mL 0.1 mM APT probe in DMF, THF and DMF/H_2O solution, respectively. 30 μL $CuSO_4$, $ZnCl_2$, $CdCl_2$, and $AlCl_3$ solutions with the concentrations of 1, 2, 3, 4, 5 mM were separately measured by added in the injection

vale at the center of the sensing chip. The fluorescence responses of each unit were recorded based on an iPhone 12 and the corresponding RGB values were extracted based on the software of Adobe Photoshop 2021.

Practical analysis of the snow sample

The A, B and C sensing units of the customized portable sensing chip were filled with 0.5 mL 0.1 mM APT probe in DMF, THF and DMF/H_2O solution, respectively. 10 mM $CuSO_4$ stock solution was diluted by the melting snow sample with the final concentrations of 1.5 and 2 mM. Then, 30 μL snow samples spiked with $CuSO_4$ were added into injection of the sensing chip. 10 mM $ZnCl_2$ stock solution was diluted by the melting snow sample with the final concentrations of 1.5 and 2 mM. Then, 30 μL snow samples spiked with $ZnCl_2$ were added into injection of the sensing chip. 10 mM $CdCl_2$ stock solution was diluted by the melting snow sample with the final concentrations of 2.5 and 3 mM. Then, 30 μL snow samples spiked with $CdCl_2$ were added into injection of the sensing chip. 10 mM $AlCl_3$ stock solution was diluted by the melting snow sample with the final concentrations of 2.5 and 3 mM. Then, 30 μL snow samples spiked with $AlCl_3$ were added into injection of the sensing chip. The fluorescence responses for the APT probe in each unit before and after detecting the above snow samples were recorded based on an iPhone 12 and the corresponding RGB values were extracted based on the software of Adobe Photoshop 2021.

Supporting Figures

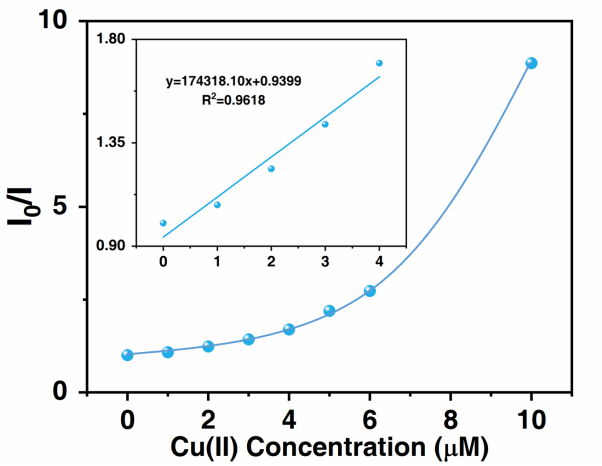

Fig. S1 Stern-Volmer curve with the doped Cu(II) concentration in the range of 0-10 μM.

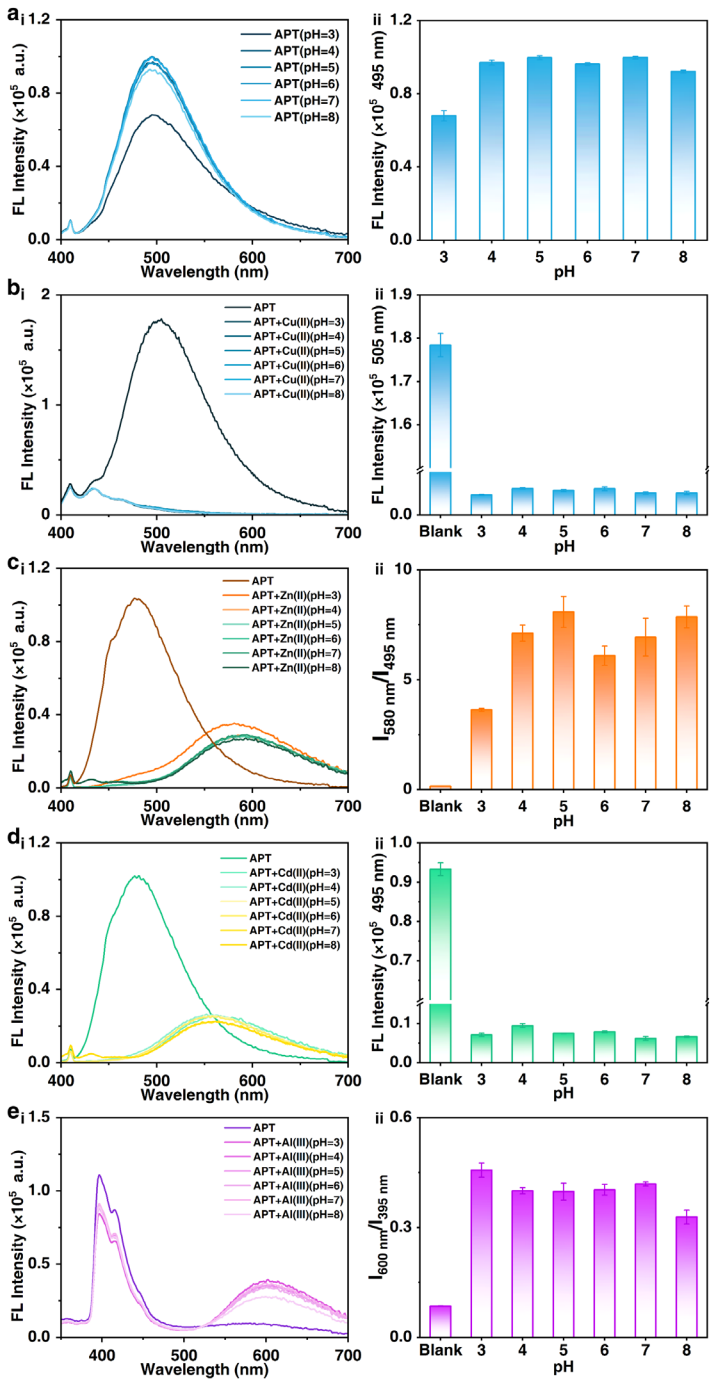

Fig. S2 Fluorescence emission of the APT probe before and after the addition of 20 μL water or metal ion solutions with pH of 3-8, the blank stands for APT probe itself without any addition.

Note: In order to evaluate the influence of the hydrogen ion concentration on the detection, a series of metal ion solutions with different pH values (3-8) were prepared for the test. It can be seen that the fluorescence emission of the probe with the addition of 20 μL water (at different pH level) did not change obvious in a pH range of 4-8, while only the addition of water with a pH of 3 induced a weakened emission, suggesting probe would not be affected in pH range of 4-8 (Fig. S2). Comparably, when the metal ion solutions with different pH levels were added in the probe solution, all the fluorescent responses with the acceptable fluctuations were obtained. These results indicated the presence of extra hydrogen ions did not greatly affect the binding of the probe towards metal ions, and the probe could be capable for detecting these metal ions with a pH range of 3-8.

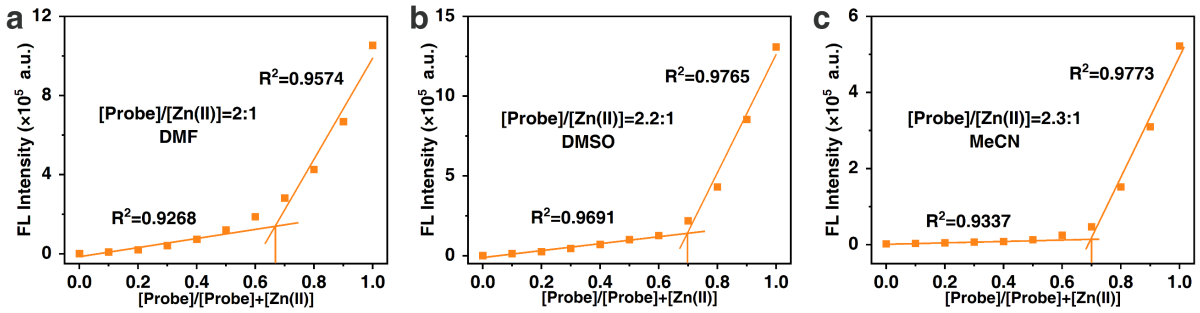

Fig. S3 (a) Job's plots of the APT probe in response to Zn(II) in i) DMF, ii) DMSO and iii) MeCN based on the fluorescence emission intensities of the APT probe.

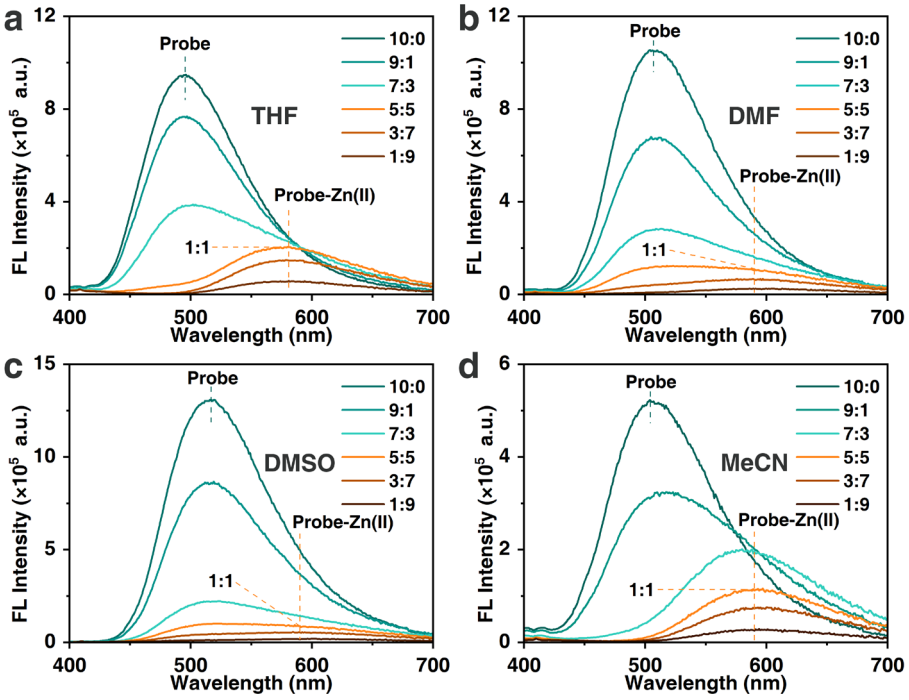

Fig. S4 Fluorescence spectra of the APT probe towards Zn(II) with the varied molar ratios in a) THF, b) DMF, c) DMSO and d) MeCN. Note: Total concentration of APT probe and Zn(II) was 0.1 mM.

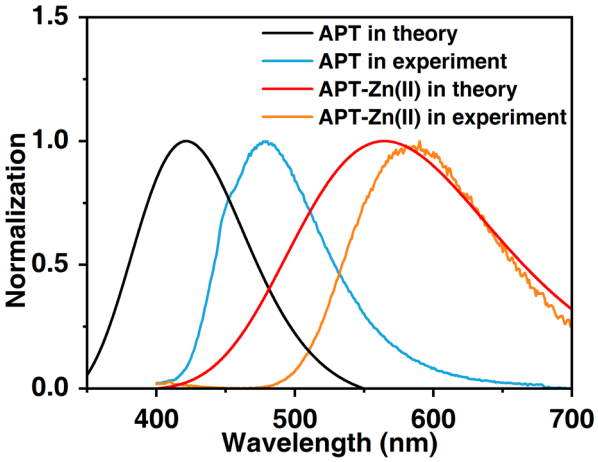

Fig. S5 Comparison of the experimental and theoretical fluorescence spectra of the APT and the APT-Zn(II).

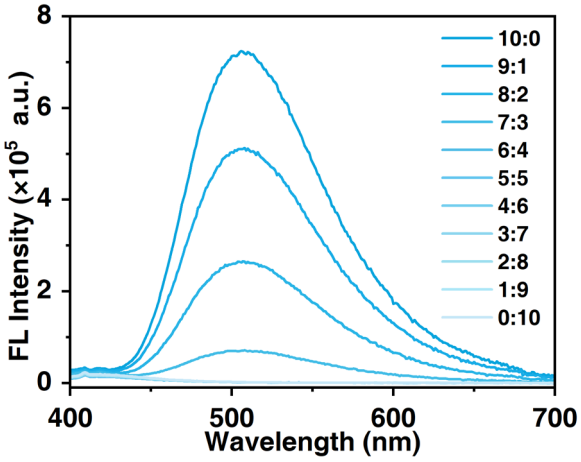

Fig. S6 Fluorescence spectra of the APT probe towards Cu(II) with the varied molar ratios in DMF.

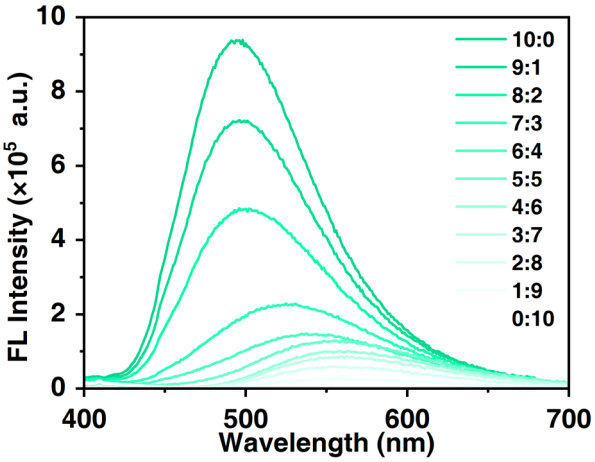

Fig. S7 Fluorescence spectra of the APT probe towards Cd(II) with the varied molar ratios in THF.

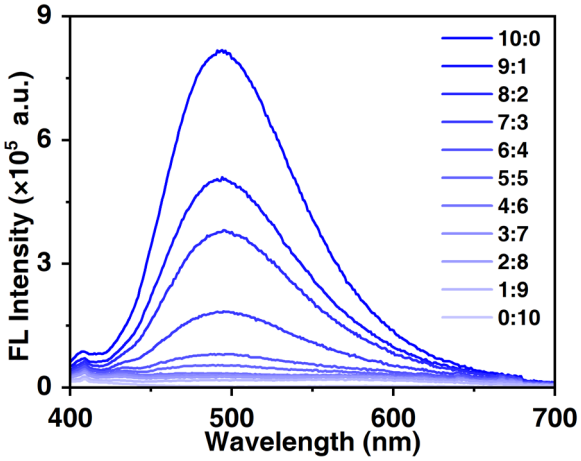

Fig. S8 Fluorescence spectra of the APT probe towards Al(III) with the varied molar ratios in THF.

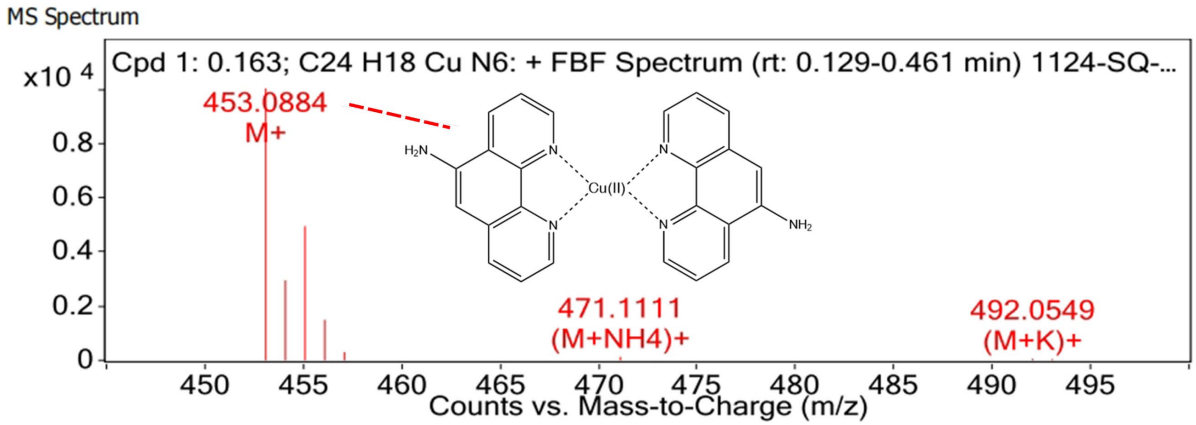

Fig. S9 HRMS spectrum of the APT-Cu(II).

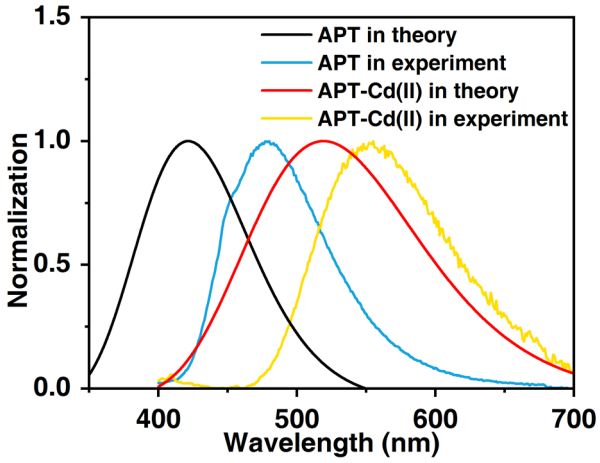

Fig. S10 Comparison of the experimental and theoretical fluorescence spectra of the APT and the APT-Cd(II).

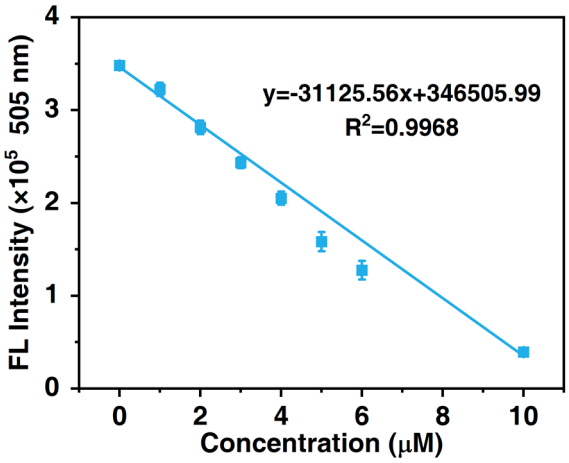

Fig. S11 Correlation curve fitted based on the fluorescence intensity at 505 nm and Cu(II) concentration.

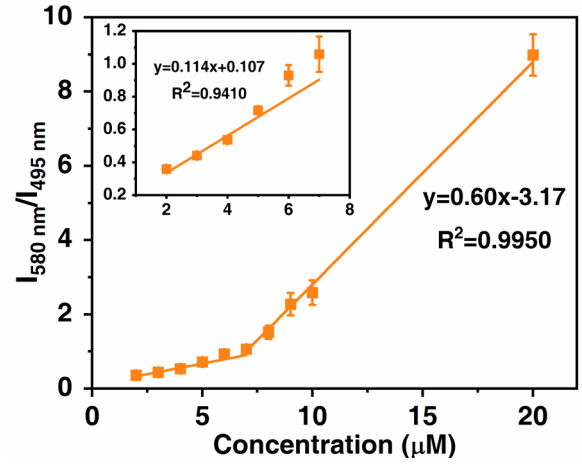

Fig. S12 Correlation curve fitted based on the fluorescence ratio (580 nm / 495 nm) and Zn(II) concentration.

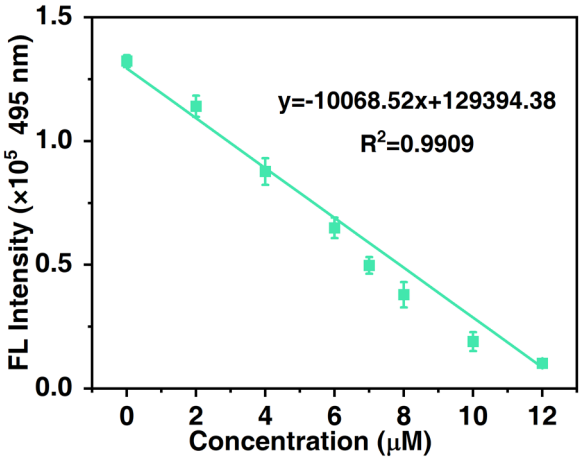

Fig. S13 Correlation curve fitted based on the fluorescence at 495 nm and Cd(II) concentration.

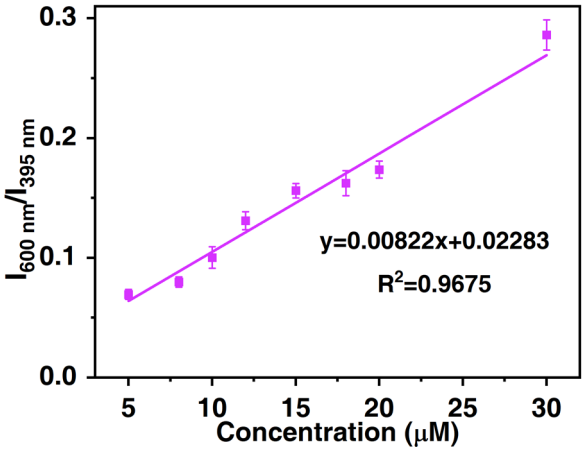

Fig. S14 Correlation curve fitted based on the fluorescence ratio (600 nm / 395 nm) and Al(III) concentration.

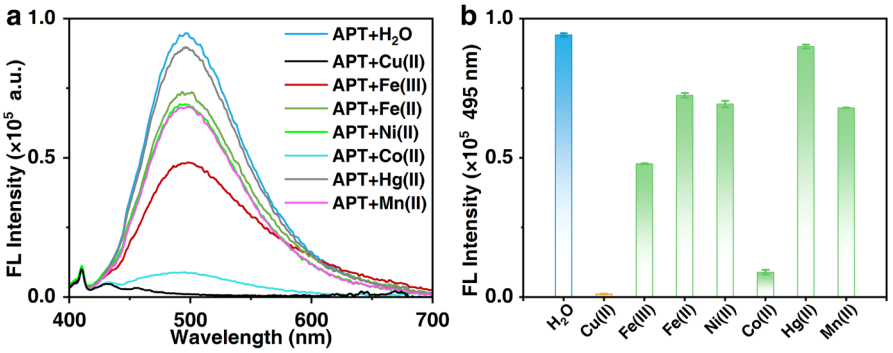

Fig. S15 (a) Fluorescence spectra of the probe in response to different metal ions, (b) histograms of the corresponding emission intensity at 495 nm.

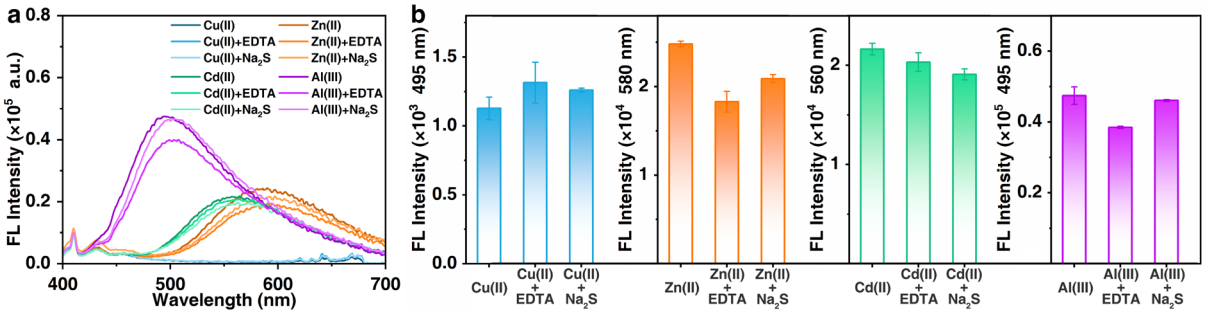

Fig. S16 (a) Fluorescence spectra of the probe in response to the metal ion, the mixture of metal ion with EDTA, and the mixture of metal ion with Na_2S, (b) histograms of the corresponding emission intensities.

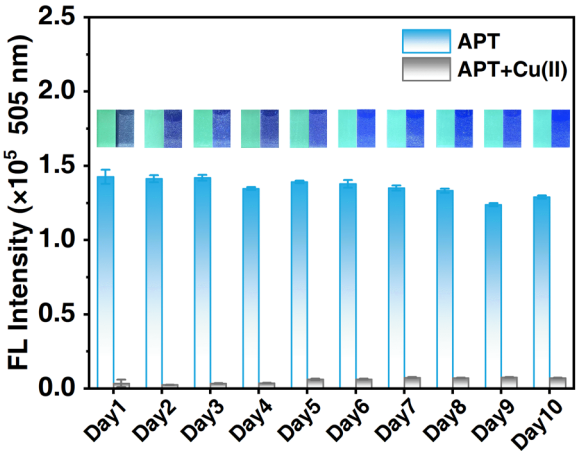

Fig. S17 Stability of the APT probe in DMF before and after detecting Cu(II) within 10 days.

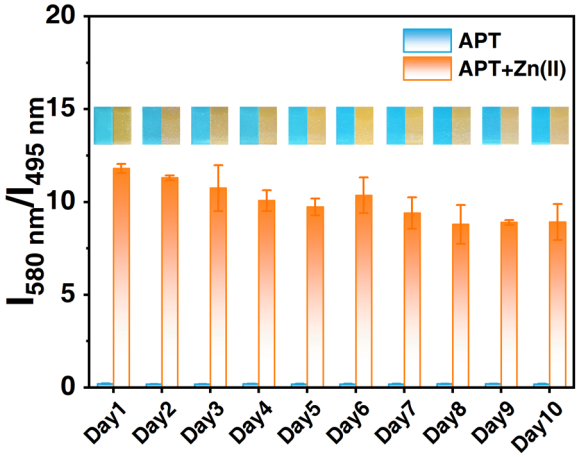

Fig. S18 Stability of the APT probe in THF before and after detecting Zn(II) within 10 days.

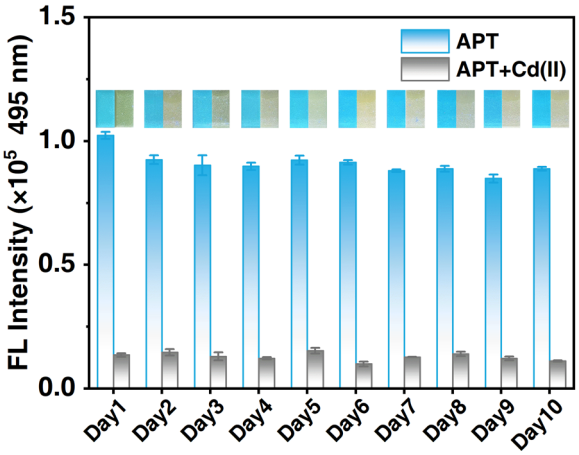

Fig. S19 Stability of the APT probe in THF before and after detecting Cd(II) within 10 days.

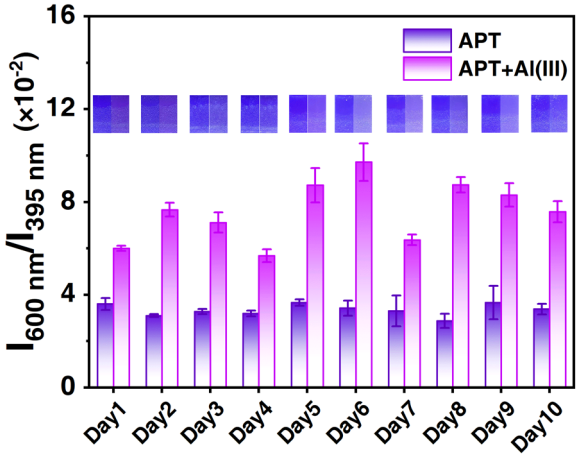

Fig. S20 Stability of the APT probe in DMF/H_2O before and after detecting Al(III) within 10 days.

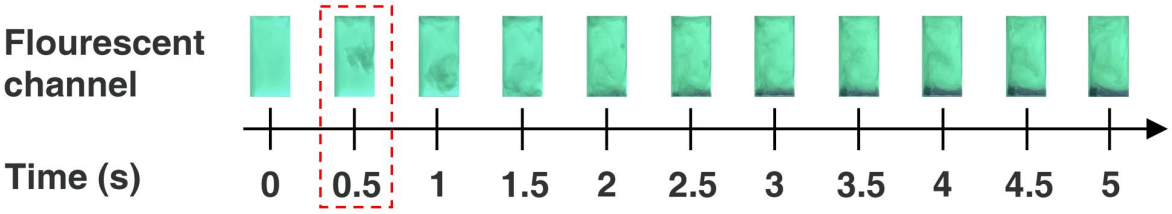

Fig. S21 Time-dependent optical images for the APT probe (in DMF) in response to Cu(II).

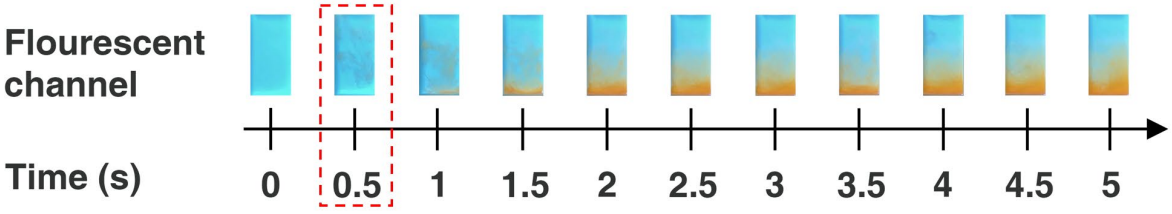

Fig. S22 Time-dependent optical images for the APT probe (in THF) in response to Zn(II).

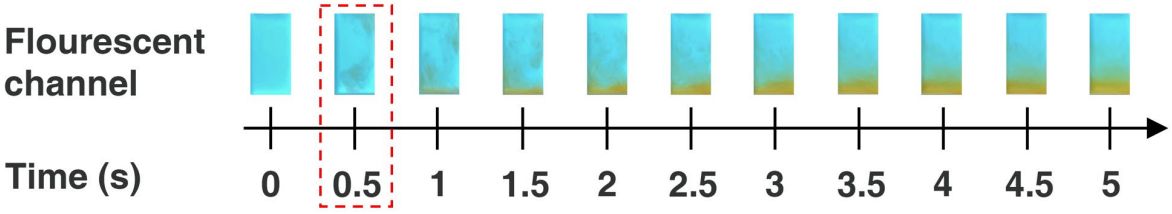

Fig. S23 Time-dependent optical images for the APT probe (in THF) in response to Cd(II).

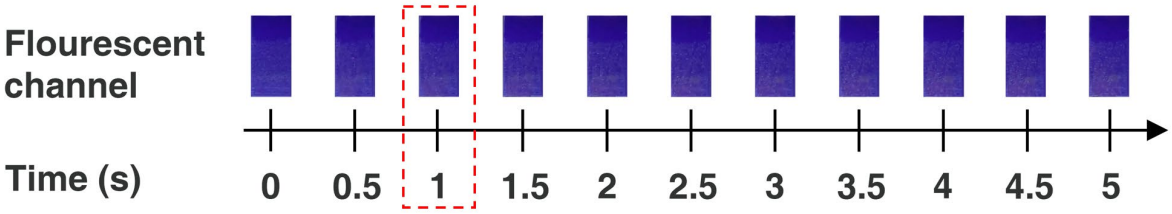

Fig. S24 Time-dependent optical images for the APT probe (in DMF/H_2O) in response to Al(III).

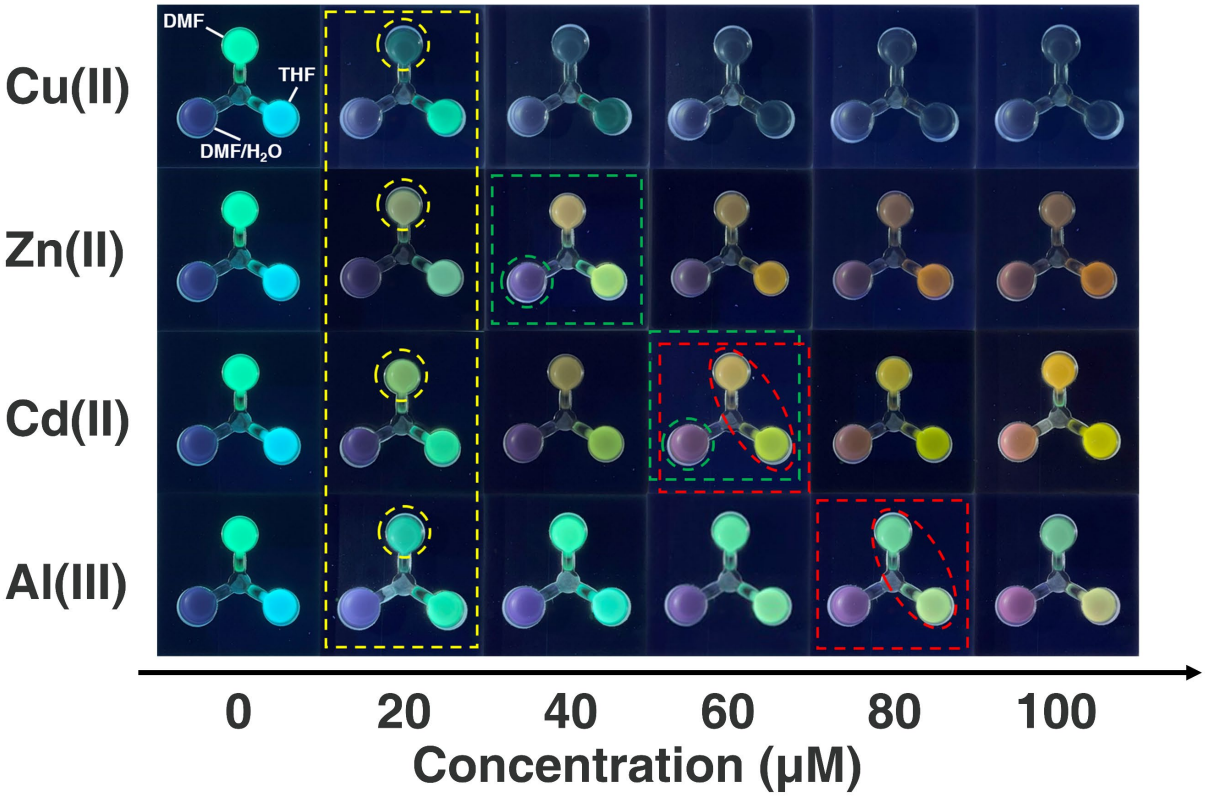

Fig. S25 Optical images of the portable sensing chip in response to target metal ions at different concentrations.

Note: In some specific cases, different metal ions at a specific concentration could induce the similar optical responses, the cross-judgment based on the three solvent systems plays an important role. For example, when the concentration of Cu(II) was at 20 μM, only the DMF channel showed obviously different quenched emission for Cu(II) (yellow dash line in Fig. S25), other two channels show similar responses to all metal ions, thus, DMF plays critical role for differentiating Cu(II) in this strategy. Furthermore, when the optical responses of the probe towards 40 μM Zn(II) and 60 μM Cd(II) were similar in channels DMF and THF, the channel of DMF/H_2O showcased a purple emission for Zn(II) and a pink emission for Cd(II) (green dash line in Fig. S25). Similarly, the combined analysis on the responses from channel DMF and THF could effectively discriminate 60 μM Cd(II) and 80 μM Al(II) when the DMF/THF channel displayed similar responses towards them (red dash line in Fig. S25).

Supporting Tables

Table S1 Physical properties of different solvents.

Solvent	Polarity	Dipole moment	Dielectric constant
THF	4.2	1.75	7.6
AC	5.4	2.9	20.6
MeCN	6.2	3.2	37.5
DMF	6.4	3.8	36.7
DMSO	7.2	3.96	46.6

Table S2 Theoretical parameters the APT probe molecule in different solvents.

Solvent	Electrostatic potential of probe (eV)	Electrostatic potential of solvent (eV)	Free energy of solvation (kcal/mol)
THF	-75.44	9.67	-16.32
DMF	-78.37	18.21	-18.21
DMSO	-78.44	16.79	-16.79

Table S3 Theoretical analysis of the binding energy between the solvent molecules and metal ions.

Metal ions	DMF	THF
Zn(II)	-23.46 kcal/mol	-16.97 kcal/mol
Cu(II)	-81.09 kcal/mol	-84.26 kcal/mol
Cd(II)	-13.11 kcal/mol	-16.70 kcal/mol
Al(III)	-245.42 kcal/mol	-229.47 kcal/mol

Table S4 Comparison of the main performances towards metal ions between the reported methods and this work.

Detection strategies	Ions	Response time	Linear range	LOD	Ref.
Fluorescence sensing	**Cu(II)**	**< 1 s**	**0-10×10^{-6} M**	**0.289×10^{-9} M**	**This work**
	Zn(II)		**0-20×10^{-6} M**	**0.16×10^{-6} M**	
	Cd(II)		**0-12×10^{-6} M**	**0.894×10^{-9} M**	
	Al(III)		**0-30×10^{-6} M**	**1.34×10^{-6} M**	
	Cu(II)	< 15 min	10-150×10^{-6} M	2.27×10^{-6} M	[12]
	Cu(II)	-	0-10×10^{-6} M	17.3×10^{-6} M	[13]
	Cu(II)		5-25×10^{-6} M	12.7×10^{-9} M	[14]
	Cu(II)		3.45-8×10^{-6} M	1.15×10^{-9} M	[15]
	Zn(II)	-	6-12×10^{-6} M	95×10^{-9} M	[16]
	Zn(II)		0-10×10^{-6} M	0.092×10^{-6} M	[17]
	Zn(II)		0-10×10^{-6} M	0.12×10^{-6} M	
	Cd(II)	-	0.8-100×10^{-6} M	0.3×10^{-6} M	[18]
	Cd(II)	1 min	0-100×10^{-9} M	0.45×10^{-9} M	[19]
	Al(III)	5 min	1-200×10^{-6} M	0.81×10^{-6} M	[20]
	Al(III)	-	0-20×10^{-6} M	39.6×10^{-9} M	[21]
Colorimetric sensing	Cu(II)	2 min	0.01-12.5×10^{-6} M	2.51×10^{-9} M	[22]
	Cu(II)	20 min	0.3-10×10^{-6} M	0.27×10^{-6} M	[23]
	Zn(II)	30 min	0-7.6×10^{-6} M	0.36×10^{-6} M	[24]
	Cd(II)	-	0-40×10^{-6} M	0.05×10^{-6} M	[25]
	Cd(II)	75 min	0.05-100×10^{-6} M	0.2×10^{-9} M	[26]
	Al(III)	< 1 min	0-30×10^{-6} M	20×10^{-6} M	[27]
Fluorescence & Colorimetric sensing	Cu(II)	< 30 s	0-3×10^{-6} M	0.14×10^{-6} M	[28]
	Zn(II)	-	0-4×10^{-6} M	0.93×10^{-6} M	

Table S5 Standards and guidelines for metal ions in drinking water recommended by the WHO.

Metal ion	WHO (mg/L)	Concentration (mol/L)
Cu(II)	2	3.2×10^{-5}
Zn(II)	3	4.5×10^{-5}
Cd(II)	0.003	2.7×10^{-8}
Al(III)	0.2	7.4×10^{-6}

Table S6 Recoveries of the APT probe in response to the metal ions in the tap-water samples and the sewage samples.

Sample	Ions	Spiked level(μM)			Found level(μM)			Recovery(±RSD%)		
Tap water	Cu(II)	4.00	6.00	10.00	4.14	6.38	10.47	103.48±4.05	106.27±1.02	104.72±0.26
	Zn(II)	3.00	5.00	15.00	2.82	5.40	15.42	94.26±2.29	108.05±1.64	102.83±2.94
	Cd(II)	4.00	8.00	12.00	4.05	8.19	11.95	101.26±4.31	102.41±0.38	99.61±0.16
	Al(III)	6.00	9.00	15.00	6.45	9.37	14.67	107.52±7.47	104.06±7.47	97.82±2.63
Sewage	Cu(II)	3.00	5.00	10.00	3.64	5.86	10.05	121.33±1.10	117.26±1.69	100.45±0.40
	Zn(II)	2.00	6.00	20.00	2.39	5.90	19.11	119.66±5.01	98.26±4.59	95.55±3.91
	Cd(II)	4.00	7.00	12.00	3.67	7.08	11.70	91.63±2.54	101.16±2.66	97.51±0.03
	Al(III)	8.00	16.00	30.00	7.58	16.04	31.88	94.71±6.98	100.24±8.75	106.27±3.29

References

1. C. Adamo and V. Barone, *The Journal of Chemical Physics*, 1999, **110**, 6158-6170.
2. S. Grimme, S. Ehrlich and L. Goerigk, *Journal of Computational Chemistry*, 2011, **32**, 1456-1465.
3. S. Grimme, *WIREs Computational Molecular Science*, 2011, **1**, 211-228.
4. F. Weigend, *Physical Chemistry Chemical Physics*, 2006, **8**, 1057-1065.
5. F. Weigend and R. Ahlrichs, *Physical Chemistry Chemical Physics*, 2005, **7**, 3297-3305.
6. Y. Zhao, N. E. Schultz and D. G. Truhlar, *Journal of Chemical Theory and Computation*, 2006, **2**, 364-382.
7. S. Miertus, E. Scrocco and J. Tomasi, *Chemical Physics*, 1981, **55**, 117-129.
8. M. J. Frisch, G. W. Trucks, H. B. Schlegel, G. E. Scuseria, M. A. Robb, J. R. Cheeseman, G. Scalmani, V. Barone, G. A. Petersson, H. Nakatsuji, X. Li, M. Caricato, A. V. Marenich, J. Bloino, B. G. Janesko, R. Gomperts, B. Mennucci, H. P. Hratchian, J. V. Ortiz, A. F. Izmaylov, J. L. Sonnenberg, Williams, F. Ding, F. Lipparini, F. Egidi, J. Goings, B. Peng, A. Petrone, T. Henderson, D. Ranasinghe, V. G. Zakrzewski, J. Gao, N. Rega, G. Zheng, W. Liang, M. Hada, M. Ehara, K. Toyota, R. Fukuda, J. Hasegawa, M. Ishida, T. Nakajima, Y. Honda, O. Kitao, H. Nakai, T. Vreven, K. Throssell, J. A. Montgomery Jr., J. E. Peralta, F. Ogliaro, M. J. Bearpark, J. J. Heyd, E. N. Brothers, K. N. Kudin, V. N. Staroverov, T. A. Keith, R. Kobayashi, J. Normand, K. Raghavachari, A. P. Rendell, J. C. Burant, S. S. Iyengar, J. Tomasi, M. Cossi, J. M. Millam, M. Klene, C. Adamo, R. Cammi, J. W. Ochterski, R. L. Martin, K. Morokuma, O. Farkas, J. B. Foresman and D. J. Fox, 2016.
9. Z. Liu, T. Lu and Q. Chen, *Carbon*, 2020, **165**, 461-467.
10. T. Lu and F. Chen, *Journal of Computational Chemistry*, 2012, **33**, 580-592.
11. W. Humphrey, A. Dalke and K. Schulten, *Journal of Molecular Graphics & Modelling*, 1996, **14**, 33-38.
12. A. Bilgic and Z. Aydin, *Journal of Colloid and Interface Science*, 2024, **657**, 102-113.
13. E. Fan, H. Guo, T. Hao, R. Zhao, P. Zhang, Y. Feng, Y. Liu and K. Deng, *Spectrochimica Acta Part A: Molecular and Biomolecular Spectroscopy*, 2023, DOI: 10.1016/j.saa.2023.123782.
14. D. Zhang, F. Xu, Q. Lu, R. Zhang and J. Xia, *Spectrochimica Acta Part A: Molecular and Biomolecular Spectroscopy*, 2023, **295**.
15. S. Wang, K. Cai, Y. Song and Y. Zhu, *ChemistrySelect*, 2021, **6**, 3788-3794.
16. S. Kumar, S. Mahata and V. Manivannan, *Journal of Photochemistry and Photobiology A: Chemistry*, 2023, DOI: 10.1016/j.jphotochem.2023.115436.
17. Y.-Z. Han, G. Tian and Q. Yang, *Inorganic Chemistry Communications*, 2023, **155**.
18. Y. Xu, C. Wang, T. Jiang, G. Ran and Q. Song, *Journal of Hazardous Materials*, 2022, **427**.
19. S. Francis and L. Rajith, *Journal of Photochemistry and Photobiology A: Chemistry*, 2024, **449**.
20. L. Peng, H. Guo, N. Wu, M. Wang, Y. Hao, B. Ren, Y. Hui, H. Ren and W. Yang, *Analytica Chimica Acta*, 2023, DOI: 10.1016/j.aca.2023.342171.
21. Y. Ding, C. Zhao, P. Zhang, Y. Cui, Y. Chen, J. Xie, W. Song, Z. Liu, Y. Ban, G. Liu and J. Yang, *Journal of Molecular Structure*, 2024, **1299**.
22. Z. Ghasemi and A. Mohammadi, *Spectrochimica Acta Part A: Molecular and Biomolecular Spectroscopy*, 2020, **239**.
23. Z. Wang, Y. Lu, J. Pang, J. Sun, F. Yang, H. Li and Y. Liu, *Microchimica Acta*, 2019, **187**.
24. S. Lee, Y.-S. Nam, H.-J. Lee, Y. Lee and K.-B. Lee, *Sensors and Actuators B: Chemical*, 2016, **237**, 643-651.
25. B. Pourbadiei, B. Eftekhari-Sis, A. Kordzadeh and A. Pourjavadi, *Heliyon*, 2023, **9**.
26. S. Ebrahim Mohammadzadeh, F. Faghiri and F. Ghorbani, *Microchemical Journal*, 2022, **179**.
27. H. Park, W. Kim, M. Kim, G. Lee, W. Lee and J. Park, *Spectrochimica Acta Part A: Molecular and Biomolecular Spectroscopy*, 2021, **245**.
28. C. Du, X. Liu, R. Li, R. Ran, X. Dong, S. Yu, H. Qi, R. Zhao, S. Yin and B. Sun, *Tetrahedron*, 2023, **144**.